European Heart Journal – Cardiovascular Imaging (2013) **14**, 331–338
doi:10.1093/ehjci/jes150

Quantification of myocardial blood flow by adenosine-stress CT perfusion imaging in pigs during various degrees of stenosis correlates well with coronary artery blood flow and fractional flow reserve

Alexia Rossi[1,2†], André Uitterdijk[2†], Marcel Dijkshoorn[1], Ernst Klotz[3], Anoeshka Dharampal[1,2], Marcel van Straten[1], Wim J. van der Giessen[2], Nico Mollet[1], Robert-Jan van Geuns[1,2], Gabriel P. Krestin[1], Dirk J. Duncker[2], Pim J. de Feyter[1,2], and Daphne Merkus[2*]

[1]Department of Radiology, Erasmus University Medical Center, Rotterdam, The Netherlands; [2]Department of Cardiology, Erasmus University Medical Center, Dr Molewaterplein 40, 3015 GD, Rotterdam, The Netherlands; and [3]Siemens Healthcare, Erlangen, Germany

Received 17 April 2012; accepted after revision 28 June 2012; online publish-ahead-of-print 26 July 2012

Aims Only few preliminary experimental studies demonstrated the feasibility of adenosine stress CT myocardial perfusion imaging to calculate the absolute myocardial blood flow (MBF), thereby providing information whether a coronary stenosis is flow limiting. Therefore, the aim of our study was to determine whether adenosine stress myocardial perfusion imaging by Dual Source CT (DSCT) enables non-invasive quantification of regional MBF in an animal model with various degrees of coronary flow reduction.

Methods and results In seven pigs, a coronary flow probe and an adjustable hydraulic occluder were placed around the left anterior descending coronary artery to monitor the distal coronary artery blood flow (CBF) while several degrees of coronary flow reduction were induced. CT perfusion (CT-MBF) was acquired during adenosine stress with no CBF reduction, an intermediate (15–39%) and a severe (40–95%) CBF reduction. Reference standards were CBF and fractional flow reserve measurements (FFR). FFR was simultaneously derived from distal coronary artery pressure and aortic pressure measurements. CT-MBF decreased progressively with increasing CBF reduction severity from 2.68 (2.31–2.81) mL/g/min (normal CBF) to 1.96 (1.83–2.33) mL/g/min (intermediate CBF-reduction) and to 1.55 (1.14–2.06) mL/g/min (severe CBF-reduction) (both $P < 0.001$). We observed very good correlations between CT-MBF and CBF ($r = 0.85$, $P < 0.001$) and CT-MBF and FFR ($r = 0.85$, $P < 0.001$).

Conclusion Adenosine stress DSCT myocardial perfusion imaging allows quantification of regional MBF under various degrees of CBF reduction.

Keywords Myocardial blood flow • Cardiac imaging • Perfusion imaging • Computed tomography (CT) • Fractional flow reserve

Introduction

Current guidelines indicate that in patients with stable angina pectoris both anatomy and functional severity of coronary obstructions should be assessed for guiding patient management.[1] Optimal medical treatment is preferred in symptomatic patients with no or moderate ischaemia, whereas revascularization is required in symptomatic patients with substantial myocardial

† Alexia Rossi and André Uitterdijk contributed equally to this work.

* Corresponding author. Tel: +31 010 7038195; Fax: +31 107044769, Email: d.merkus@erasmusmc.nl

ischaemia,[2–4] and percutaneous coronary intervention (PCI) is recommended for lesions with impaired fractional flow reserve (FFR) in patients with multi-vessel disease.[5–8]

Coronary CT angiography (CTA) is a well-established, non-invasive imaging modality for detection and ruling-out coronary atherosclerosis.[9–11] Coronary CTA however, cannot accurately predict whether an intermediate lesion is flow limiting therefore requiring the use of additional functional testing.[12,13] Yet, little information is available about the ability to use CT for the quantitative assessment of myocardial blood flow (MBF) at different levels of coronary artery stenosis. Only few preliminary experimental studies demonstrated the feasibility of adenosine stress CT myocardial perfusion to determine absolute MBF, thereby providing information about the functional severity of coronary lesions.[2,14,15]

The purpose of our study was two-fold: (i) to quantify regional CT-derived MBF (CT-MBF) at different degrees of coronary flow reduction in a well-established large animal model; (ii) to correlate CT-MBF with the coronary artery blood flow (CBF), the experimental reference standard, and with FFR, the clinical reference standard.

Methods

Animal preparation

All procedures were conducted in compliance with the *Guide for the Care and Use of Laboratory Animals* (NIH Publication No. 85–23 revised 1996), and with prior approval of the Animal Care Committee of our institution. Nine, 5–6 months old, crossbred Yorkshire X Landrace swine (34.2 ± 3.6 kg) were sedated with an i.m. injection of ketamine (20 mg/kg, Anisane, Raamsdonksveer, The Netherlands), midazolam (1 mg/kg, Actavis, Baarn, The Netherlands), and atropine sulphate (1 mg, Pharmachemie, Haarlem, The Netherlands). Anaesthesia was induced with an i.v. injection of pentobarbital sodium (15 mg/kg, Faculty of Veterinary Medicine, Utrecht, The Netherlands). Animals were intubated and mechanically ventilated with a mixture of O_2 and N_2 (1:2 v/v).[16] Anaesthesia was maintained by i.v. pentobarbital sodium infusion (15 mg/kg/h). A left thoracotomy was performed in the fourth intercostal space and the pericardium was opened. Fluid-filled polyvinylchloride catheters were placed into the aortic arch, for the measurement of pressure and for blood gas analysis to maintain blood gases within the physiological range. Catheters were also placed in the pulmonary artery for the infusion of drugs and contrast material. Subsequently, the left anterior descending coronary artery (LAD) was dissected free for the placement of a flow probe (Transonic Systems Europe B.V., Maastricht, The Netherlands) and a remote controlled silicone hydraulic vascular occluder (Fine Science Tools GmbH, Heidelberg, Germany). In addition, a fluid-filled polyvinylchloride angiocatheter for the measurement of distal coronary pressure and determination of FFR was inserted into the LAD distal to the occluder. Flow probe, occluder, and catheters were exteriorized, the chest was closed and anaesthetized animals were transported to the CT suite using a mobile ventilator (Carina™, Dräger Medical, Best, The Netherlands).

Experimental and CT imaging protocols

A dual source CT (DSCT) scanner (SOMATOM Definition Flash, Siemens Healthcare, Forchheim, Germany) was used for perfusion imaging. All animals were placed in the supine position. First, animals underwent DSCT myocardial perfusion imaging at rest. Subsequently, DSCT myocardial perfusion imaging was performed during maximal vasodilation. Maximal vasodilation was obtained with intravenous infusion of 500 μg/kg/min adenosine (Adenoscan, Sanofi-Aventis Frankfurt, Germany). At this dose, adenosine resulted in marked systemic vasodilation and hypotension. To maintain blood pressure, the α_1-adrenoceptor agonist phenylephrine was co-infused (~5 μg/kg/min i.v., Pharmacy Erasmus MC, Rotterdam, The Netherlands) with adenosine. Since swine lack significant α_1-adrenergic coronary microvascular constrictor responses,[17] phenylephrine can be used to oppose the systemic effects of adenosine, while leaving adenosine-induced coronary vasodilation unperturbed.[16] Under maximal vasodilation the hydraulic occluder was manually inflated to sequentially obtain at least one intermediate degree of flow-limiting coronary stenosis and at least one severe degree of flow-limiting stenosis. Total occlusion was performed to delineate the LAD perfusion territory. CT perfusion imaging was repeated at each severity level of flow reduction using a novel electrocardiogram (ECG)-triggered dynamic scan mode. All scans were performed in cranio-caudal direction during end-expiratory breath-hold obtained by interrupting the mechanical ventilator. The data were acquired at two alternative table positions while the table was moving back and forth.[18] Image acquisition was triggered at 200 ms after the R-wave. The scan coverage was 73 mm resulting from a detector width of 38.4 mm and 10% overlap between both scan ranges. The minimum cycle time for the alternating scan is 950 ms. For the range of heart rates in this study, we acquired data every second or third heart beat. Hence, volume scan of the total heart was obtained every 2–3 s. The tube voltage was 100 kV for each X-ray tube and the total tube current-time product was 300 mAs/rot. Prior to each scan 36 mL of contrast material (Ultravist 370, Bayer Schering Pharma, Berlin, Germany) was injected through a pulmonary artery catheter at a flow rate of 6 mL/s, followed by a saline chaser of 30 mL at 6 mL/s. Data acquisition started 2 s before the contrast medium injection and lasted for 30 s. The delay between two consecutive scans was 20 min. Depending on the heart rate, the CTDIvol ranged from 115.1 to 168.5 (mean 149.5 ± 14.1) mGy. The corresponding dose-length product was 844.0–1129.0 (mean 1012.2 ± 80.0) mGycm.

During each experiment heart rate, aortic pressure, mean coronary artery pressure, and CBF were continuously recorded (Codas, DATAQ) and stored for off-line analysis using a custom written software in MatLab (the Math Works). FFR was calculated as the ratio of distal coronary artery pressure and aortic pressure.

At the end of the experiment, animals were sacrificed with an i.v. overdose of pentobarbital sodium.

Data analysis

All CT images were evaluated by one cardiac radiologist with 4-years experience in cardiac imaging (A.R.). To assess intra- and inter-observer agreement, the MBF of the ischaemic myocardial territories was measured on 10 randomly chosen CT data sets by two independent observers (A.R. and A.D.). One observer (A.R.), who was blinded to the previous results, measured the data sets twice, separated by at least 12 weeks. Both observers were blinded to all CBF and FFR measurements.

CT images were reconstructed with a slice thickness of 3 mm and an increment of 1.5 mm using a medium-smooth kernel (B30f). The dynamic data were analysed using commercial software, volume perfusion CT body on a standard workstation (MMWP, Siemens Healthcare, Germany). Reconstruction and post-processing analysis of the CT perfusion images was previously described.[14] Briefly, the left ventricular myocardium was segmented manually placing a volume of interest (VOI) and using a combination of a system of blood pool removal

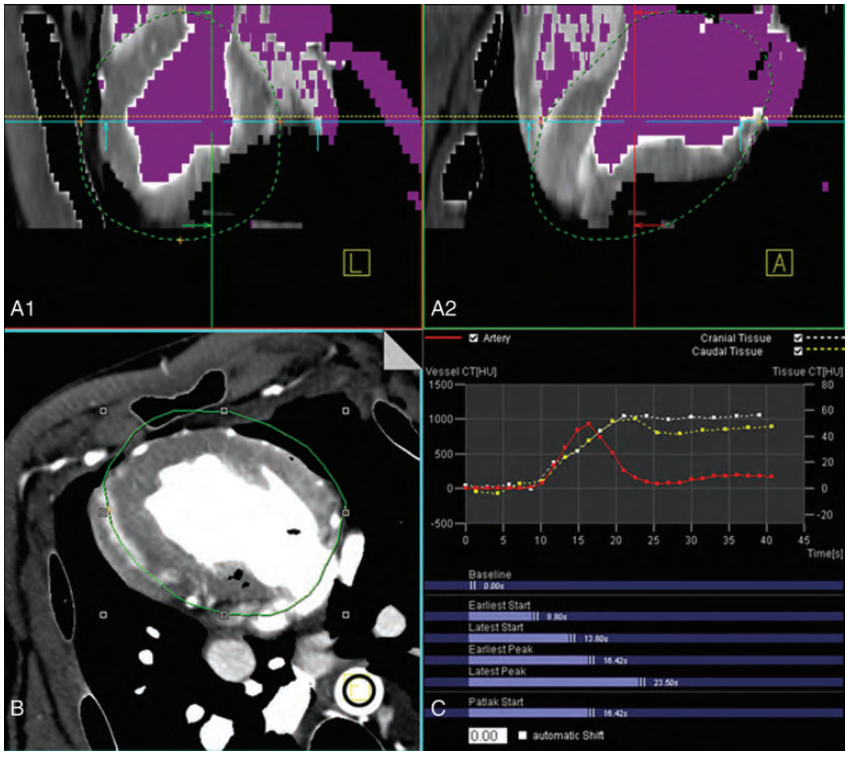

Figure 1 CT-perfusion imaging post-processing. (*A1*) and (*A2*) show the segmentation of the left ventricle. The left ventricle myocardium is isolated using in combination a Hounsfield unit-based thresholding and a peak enhancement analysis within a volume of interest, VOI (green line). The arterial input function is sampled from two regions of interest placed in the descending aorta of the cranial (*B*) and caudal part of the image stack. One arterial input function is then obtained (red time–attenuation curve, TAC) in (*C*) combining the information of both ROIs.

and HU thresholding (*Figure 1A*). Afterwards, the arterial input function was sampled drawing a region of interest (ROI) in the descending aorta at the cranial and the caudal ends of the two image stacks (*Figure 1B*). The data from both ROIs were then combined into one arterial input function (*Figure 1C*) and time attenuation curves (TACs) were built for each voxel within the VOI. A dedicated parametric deconvolution technique based on a two-compartment model of intra- and extravascular space was applied to fit the TACs (*Figure 2 B1* and *B2*). CT-MBF in mL/100 mL/min of each voxel was then calculated using the maximum slope of the fit curves and quantitative three-dimensional colour maps representing the MBF distribution in the myocardium were generated (*Figure 2A*). CT myocardial perfusion in mL/g/min was calculated assuming a myocardium specific density of 1.05 g/mL.

The LAD perfusion territory of each animal was first defined using the colour code MBF maps during total occlusion of the LAD. Afterwards a VOI was manually placed in the most representative ischaemic area of the LAD territory for each degree of CBF reduction within the same animal. A VOI was manually drawn also in the remote myocardium (inferior wall). CT-MBF was then obtained for both regions.

Statistical analysis

Statistical analysis was performed using a dedicated statistical software program (SPSS PASW, version 17.0.2, IMB, Chicago, IL, USA). Measurements are presented as median (inter-quartile range). All measurements were pooled and afterwards classified in three groups according to CBF: no-CBF reduction, intermediate CBF reduction (range: 15–39%), and severe CBF reduction (range: 40–95%). When CBF measurements were not available the classification in different groups was based on FFR measurements. All measurements at rest and during maximal vasodilation were compared using the Wilcoxon signed-rank test. For each degree of coronary flow reduction, CT-MBF was compared between the ischaemic and remote myocardial territories using the Wilcoxon signed-rank test. CT-MBF, CBF, and FFR were compared between different degrees of CBF reduction applying the Kruskal–Wallis test for multiple independent samples. The Mann–Whitney test was applied for *post hoc* comparison. Correlation analysis was performed to evaluate the association between CT-MBF and CBF and FFR. Linear regression models were then fitted to asses the value of CT-MBF to predict CBF and FFR.

A P-value < 0.05 was considered statistically significant.

Results

Two pigs died before CT imaging due to ventricular fibrillation. In seven animals, instrumentation and CT myocardial perfusion imaging were successfully performed, and a total of 32 data sets were obtained. One CT data set was excluded because of poor image quality. In one pig (4 datapoints), measurements of FFR could not be obtained due to a clot in the coronary artery catheter. Owing to probe malfunction (lack of contact between probe and vessel), 11 measurements of CBF could not be

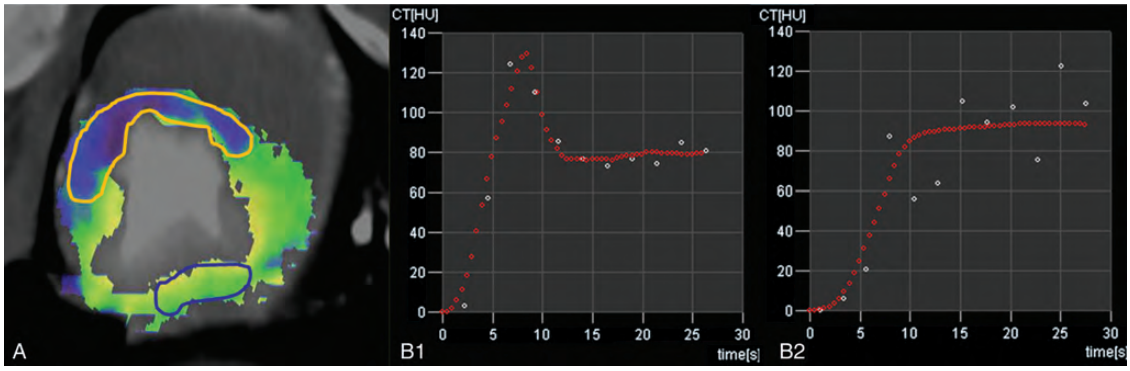

Figure 2 Ischaemic and remote myocardial territory. Quantitative three-dimensional colour-map representing the distribution of myocardial blood flow (*A*). During maximal vasodilation the ischaemic anterior wall shows reduced perfusion (blue area), whereas the normal myocardium appears greenish (remote myocardium). A dedicated parametric deconvolution technique based on a two compartment model of intra- and extra-vascular space was used to fit the TACs in a representative normal (*B1*) and ischaemic (*B2*) myocardium. The white dots are the measured enhancement values. The upslope of the time attenuation curve of the ischaemic myocardium is less steep compared to the remote myocardium.

Table 1 Number of data sets included in the analysis

Pigs\data sets	CT	FFR	CBF
CT	7 p\31 ds	28 ds	20 ds
FFR	6 p	6 p\28 ds	17 ds
CBF	5 p	4 p	5 p\21 ds

p, number of pigs; ds, number of data sets.

obtained. Consequently, a total of 21 CBF measurements, 28 FFR measurements, and 31 CT data sets obtained in 7 swine were analysed (*Table 1*).

At maximal vasodilation, a homogeneous increase in MBF was observed throughout the entire myocardium (*Figure 3*). At each level of CBF reduction, the ischaemic region in the LAD territory was clearly visible as defect in the colour MBF maps in all seven animals. Moreover, a progressive increase of the size of the ischaemic territory was observed in each animal with increasing the severity of CBF reduction.

Haemodynamic parameters

Despite the infusion of phenylephrine, blood pressure decreased from 96 (87–100) mmHg at baseline to 88 (78–99) mmHg during the infusion of adenosine, whereas heart rate increased from 100 (90–145) to 136 (117–154) b.p.m. Animals showed a slight haemodynamic deterioration with increasing severity of coronary flow reduction as shown by the progressive decrease in aortic pressure (*Table 2*).

CT-MBF of ischaemic and remote myocardium

During normal coronary arterial inflow, maximal vasodilation with adenosine resulted in a 2.8-fold increase in CT-MBF from 0.99 (0.95–1.30) mL/g/min to 2.76 (2.47–3.65) mL/g/min ($P = 0.001$) and a 3.7-fold increase in CBF, from 40 (25–83) mL/min to 149 (135–170) mL/min ($P = 0.006$).

In all swine, CT-MBF of the ischaemic territory decreased progressively with increasing severity of stenosis ($P < 0.001$; *Table 2*). A typical response of CT-MBF to progressive flow reductions is presented in *Figure 3*. CT-MBF of ischaemic myocardial territories was markedly lower than CT-MBF of the remote myocardium ($P < 0.001$) at severe CBF reduction.

CT-MBF correlated strongly with absolute flow measurement represented by CBF during no and various levels of CBF reduction ($r = 0.85$, $P < 0.001$ *Figure 4A*). CT-MBF showed a similarly strong correlation with FFR ($r = 0.85$, $P < 0.001$) (*Figure 4B*).

Intra- and inter-observer agreement

The mean difference (measure of precision) of CT-MBF was 0.07 mL/g/min with a standard deviation (measure of accuracy) of 0.18 mL/g/min for intra-observer measurements ($r = 0.96$; $P < 0.001$). The mean difference ($\pm$standard deviation) for inter-observer measurements was 0.10 ($\pm$0.40) mL/g/min ($r = 0.764$; $P = 0.006$).

Discussion

The present study assessed the diagnostic accuracy of stress dynamic DSCT quantification of MBF in ischaemic and remote myocardium in a large animal model with controlled reduction in CBF under maximal vasodilation (from normal to moderate to severe CBF reduction) compared with the experimental reference standard, CBF, and the clinical reference standard, FFR measurements. The major finding was that adenosine stress dynamic DSCT perfusion imaging provided regional quantification of MBF of ischaemic and remote myocardium under experimental conditions, which correlated very well with CBF and FFR.

Table 2 Haemodynamic parameters and CBF, FFR, and CT-MBF of ischaemic and remote myocardium during different levels of coronary blood flow, CBF, at the time of CT acquisition

CBF reduction (range%)	No (0%)	Intermediate (15–39%)	Severe (40–95%)	*P*-value*
HR (b.p.m.)	136 (117–154)	129 (118–147)	128 (116–143)	0.788
AoP (mmHg)	88 (78–99)	89 (86–94)	82 (74–91)	0.269
Distal CAP (mmHg)	80 (65–91)	73 (66–80)	44 (37–62)** ***	0.002
Distal CBF (mL/min)	148 (135–170)	116 (113–125)**	61 (30–83)** ***	<0.001
FFR	0.90 (0.84–1.00)	0.76 (0.65–0.91)	0.60 (0.51–0.69)** ***	<0.001
CT-MBF- ischaemic (mL/g/min)	2.68 (2.31–2.81)	1.96 (1.83–2.33)**	1.55 (1.14–2.06)** ****	<0.001
CT-MBF-remote (mL/g/min)	2.76 (2.47–3.65)	2.51 (2.03–3.05)	3.02 (2.79–3.68)	0.162

Data are presented as median and inter-quartile range.
HR, heart rate; AoP, aortic pressure; CAP, coronary artery pressure; CBF, coronary artery blood flow; FFR, fractional flow reserve; CT-MBF, CT-derived myocardial blood flow.
**P*-value between CBF reduction groups (Kruskal–Wallis test).
***P*-value < 0.05 vs. no CBF reduction (Mann–Whitney test).
****P*-value < 0.05 severe vs. intermediate CBF reduction (Mann–Whitney test).
*****P*-value < 0.05 between CT-MBF of the LAD ischaemic territory and CT-MBF of the remote myocardium (Wilcoxon signed-rank test).

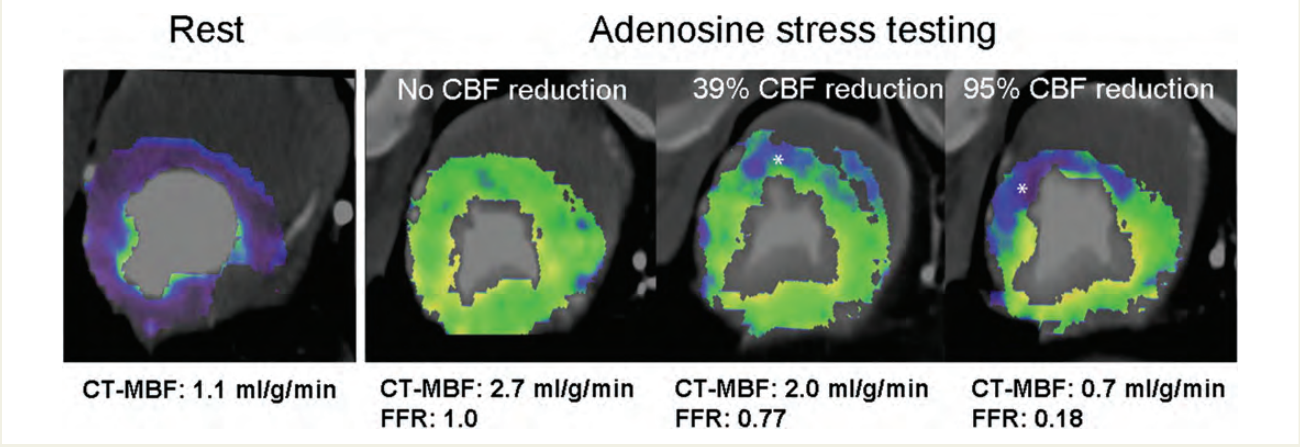

Figure 3 The response of the CT-derived myocardial blood flow (CT-MBF) to different levels of coronary blood flow (CBF) reduction. Example of CT-MBF colour maps of the myocardium during maximal vasodilation, intermediate CBF reduction, and severe CBF reduction. The ischaemic area (*) is well visible in the colour map. A progressive decrease in CT-MBF occurs with increasing severity of CBF reduction.

CT quantification of MBF

Static myocardial perfusion imaging during adenosine stress has been recently investigated in humans and shows a diagnostic accuracy comparable with SPECT to detect significant coronary stenoses.[19,20] However, static perfusion imaging provides only qualitative information of the myocardial perfusion by comparing the attenuation of the ischaemic area to the attenuation of the remote myocardium. Quantification of myocardial perfusion is possible using dynamic CT scanning and it was already investigated by electron beam CT (EBCT) in the late 1980's. EBCT was a remarkable technical development with an excellent temporal resolution allowing dynamic perfusion imaging but was limited by a rather small coverage and thick slices. Nevertheless, studies in animal models[21] and healthy humans[22] reported good correlations between EBCT-derived MBF vs. microspheres[21] and vs. indicator dilution methods,[22] respectively. EBCT technology has been replaced by multidetector CT technology and, due to improved temporal resolution and coverage, the latest generation scanners now allow quantitative myocardial perfusion imaging.[23] Thus, George *et al.*[15] proved the ability of CT to quantify MBF in an experimental model using 64-multidetector CT. Mahnken *et al.*[14] and Bamberg *et al.*[24] showed the feasibility of a novel ECG-triggered dynamic shuttle-mode scan with data being acquired at two alternating table positions in the quantification of MBF in animal and human studies, respectively. The use of two alternating table positions increased the scan coverage and the presence of two X-rays tubes provided a better temporal resolution when compared with 64-multidetector CT. The main criticism of studies so far has been that CT-MBF underestimates MBF. We observed a higher CT-MBF in the ischaemic as well as in the remote myocardium than Mahnken *et al.*,[14] and Bamberg *et al.*[24] which can be explained by the higher dose of adenosine in our study (500 μg/kg/min) when

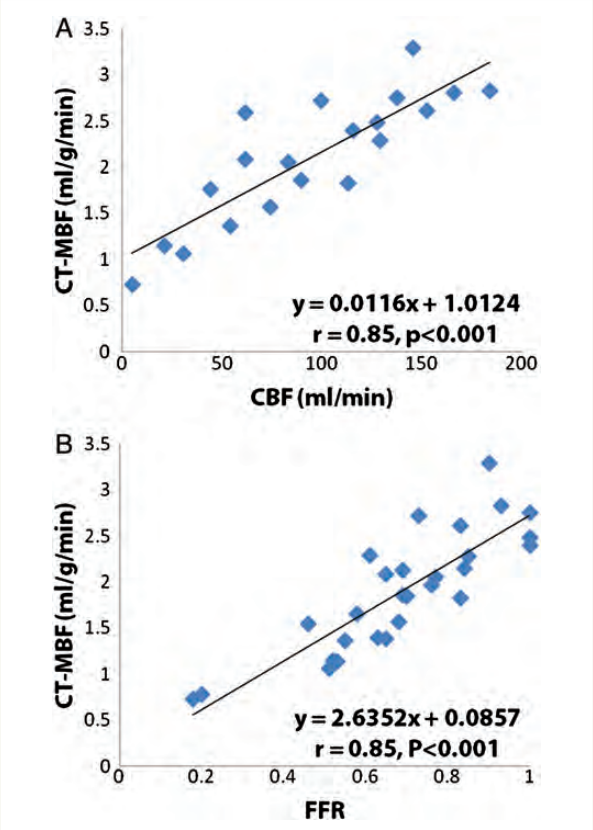

Figure 4 CT-derived myocardial blood flow (CT-MBF) vs. coronary blood flow (CBF) and fractional flow reserve (FFR).

compared with Mahnken *et al.*[14] (240 μg/kg/min) and to Bamberg *et al.*[24] (140 μg/kg/min), in conjunction with the use of phenylephrine resulting in a relatively well-maintained aortic blood pressure during adenosine infusion in our study. Additionally, in our study the 6 s contrast bolus was injected directly into the pulmonary artery instead of a 10 s bolus into a peripheral ear vein. This yielded a much better defined arterial input function with better tissue discrimination and more accurate modelling. The values of MBF may differ in humans because a peripheral venous access is commonly used for contrast injection.

Comparison of CT-MBF with CBF and FFR

In our study, we found an excellent correlation between CT-MBF and the experimental reference standard, CBF, over a wide range of blood flows. In our experimental set-up, CBF provided a direct measurement of the blood flow distal to a coronary stenosis produced by the occluder but direct measurements of CBF are not available in the clinical environment, although coronary blood velocity can be measured using a flow wire. Clinically, FFR was therefore introduced as indirect parameter of myocardial perfusion. FFR has been well established as an accurate, yet invasive, parameter to assess the functionality of a coronary stenosis independent from heart rate, blood pressure, and left ventricular function. In the present study, we found a good correlation between CT-MBF and FFR over a wide range of coronary flow reductions, suggesting that absolute MBF measurements with CT can provide clinically relevant information about stenosis severity. Indeed, Bamberg *et al.*[24] recently showed the feasibility of dynamic CT perfusion imaging for the detection of haemodynamically significant coronary artery stenoses, as defined with FFR, in a human study. These authors found a cut-off point of 75 mL/100 mL/min to provide the highest discriminatory power between haemodynamically significant and non-significant coronary artery lesions. This cut-off value needs further validation in different patient populations after a standardized CT protocol has been developed.

Limitations

Our study has some limitations that are either related to our animal model or are more general limitations of CT technology.

Animal model

First, our study was designed as a feasibility study using a relatively small number of animals. Yet, the use of multiple measurements per animal and the well-defined experimental conditions make the results reliable and reproducible as further evidenced by high correlation between CT-MBF, CBF, and FFR . Secondly, we did not use microspheres as experimental gold standard for an *in vivo* measurement of MBF. Bamberg *et al.*[25] provided good correlation between CT-MBF and microsphere-derived myocardial flow in the pig model of LAD obstruction using the same CT technology. Thirdly, our experimental set-up was designed as a single vessel LAD obstruction, therefore our results cannot be extrapolated to multi-vessel coronary artery disease. Nevertheless, we expect that this CT technology will give good results also in the situation of three vessel disease because it provides an absolute quantification of regional MBFs rather than relative flows as obtained in SPECT imaging. Fourthly, the pigs (mean weight ± standard deviation: 34.2 ± 3.6 kg) were relatively small compared with adult humans, which may imply the need to use higher kV and mAs settings during the CT acquisition in humans. However, in a recent study performed in patients, Bamberg *et al.*[24] used successfully 100 kV and 300 mAs as we used in pigs.

CT-technology

There are several technical aspects that need further consideration. (i) An important technical limitation is the volume coverage; 64-slice CT scanners used to be limited to a single detector up to 40 mm that was not sufficient to cover the whole heart. Nowadays two alternatives are available: first, a CT system with 320 rows that can cover the whole heart in one gantry rotation,[26–28] the second alternative is the shuttle mode acquisition used in our study. Although the acquisition coverage of the shuttle mode technique of 73 mm was sufficient for encompassing the entire heart of the pigs, this coverage may be not sufficient in humans, even when triggering in the systolic phase, due to the larger size of the human heart. Indeed Bamberg *et al.*[24] found that one-third of the scans provided incomplete coverage of the myocardium. Thus, further improvements in CT technology should aim in increasing the coverage along the *z*-axis. (ii) We used central venous access for contrast injection, which provides a tighter input function and likely results in higher values of MBF. These values may not be

reproducible in patients because a peripheral venous access is commonly used in the clinical routine. (iii) The addition of dynamic perfusion CT imaging to the conventional clinical cardiac CTA protocol will increase the total amount of radiation dose. Optimization of radiation dose reduction protocols should be developed with the preservation of image quality. (iv) Finally, iodinated contrast medium in the left ventricular cavity can negatively affect the assessment of myocardial perfusion. However, this may be circumvented by using beam-hardening artefact correction algorithms to increase the accuracy of CT perfusion imaging in the quantification of MBF.[29]

Clinical implications and challenges

Our study shows that CT myocardial perfusion imaging can quantitatively measure MBF in experimental animals, and thereby can be used to assess stenosis severity. This observation is supported by a few small-sized studies showing that CT myocardial perfusion imaging is also feasible in patients.[24,26,30–32]Thus, the addition of CT myocardial perfusion imaging to the standard coronary CTA provides complementary anatomical and functional information in a single, non-invasive examination which improves patient management. Future improvements in CT technology, aimed at increasing the coverage and reducing the radiation exposure, would facilitate implementation of this non-invasive imaging technique in clinical practice.

Conclusions

The present study demonstrates that dynamic dual source CT can identify regional reductions of MBF, during pharmacological coronary vasodilation, over a wide range of flow-limiting coronary artery obstruction severities with a good correlation with CBF and FFR.

Acknowledgements

We would like to dedicate this manuscript to Prof. Wim van der Giessen who sadly passed away in June 2011.

Funding

This research was partially financed by, and Volume Perfusion CT software was provided by, Siemens Nederland, Healthcare Sector, under a Cooperation Agreement.

Conflict of interest: E.K. is employed by Siemens Healthcare. Siemens also provided partial funding and free access to Volume Perfusion CT software.

References

1. Fox K, Garcia MA, Ardissino D, Buszman P, Camici PG, Crea F *et al.* Guidelines on the management of stable angina pectoris: executive summary: The Task Force on the Management of Stable Angina Pectoris of the European Society of Cardiology. *Eur Heart J* 2006;**27**:1341–81.
2. Shaw LJ, Berman DS, Maron DJ, Mancini GB, Hayes SW, Hartigan PM *et al.* Optimal medical therapy with or without percutaneous coronary intervention to reduce ischemic burden: results from the Clinical Outcomes Utilizing Revascularization and Aggressive Drug Evaluation (COURAGE) trial nuclear substudy. *Circulation* 2008;**117**:1283–91.
3. Hachamovitch R, Hayes SW, Friedman JD, Cohen I, Berman DS. Comparison of the short-term survival benefit associated with revascularization compared with medical therapy in patients with no prior coronary artery disease undergoing stress myocardial perfusion single photon emission computed tomography. *Circulation* 2003;**107**:2900–7.
4. Boden WE, O'Rourke RA, Teo KK, Hartigan PM, Maron DJ, Kostuk WJ *et al.* Optimal medical therapy with or without PCI for stable coronary disease. *N Engl J Med* 2007;**356**:1503–16.
5. Legalery P, Schiele F, Seronde MF, Meneveau N, Wei H, Didier K *et al.* One-year outcome of patients submitted to routine fractional flow reserve assessment to determine the need for angioplasty. *Eur Heart J* 2005;**26**:2623–9.
6. Pijls NH, van Schaardenburgh P, Manoharan G, Boersma E, Bech JW, van't Veer M *et al.* Percutaneous coronary intervention of functionally nonsignificant stenosis: 5-year follow-up of the DEFER Study. *J Am Coll Cardiol* 2007;**49**:2105–11.
7. Tonino PA, De Bruyne B, Pijls NH, Siebert U, Ikeno F, van' t Veer M *et al.* Fractional flow reserve versus angiography for guiding percutaneous coronary intervention. *N Engl J Med* 2009;**360**:213–24.
8. Pijls NH, Fearon WF, Tonino PA, Siebert U, Ikeno F, Bornschein B *et al.* Fractional flow reserve versus angiography for guiding percutaneous coronary intervention in patients with multivessel coronary artery disease: 2-year follow-up of the FAME (Fractional Flow Reserve Versus Angiography for Multivessel Evaluation) study. *J Am Coll Cardiol* 2010;**56**:177–84.
9. Budoff MJ, Dowe D, Jollis JG, Gitter M, Sutherland J, Halamert E *et al.* Diagnostic performance of 64-multidetector row coronary computed tomographic angiography for evaluation of coronary artery stenosis in individuals without known coronary artery disease: results from the prospective multicenter ACCURACY (Assessment by Coronary Computed Tomographic Angiography of Individuals Undergoing Invasive Coronary Angiography) trial. *J Am Coll Cardiol* 2008;**52**:1724–32.
10. Meijboom WB, Meijs MF, Schuijf JD, Cramer MJ, Mollet NR, van Mieghem CA *et al.* Diagnostic accuracy of 64-slice computed tomography coronary angiography: a prospective, multicenter, multivendor study. *J Am Coll Cardiol* 2008;**52**:2135–44.
11. Miller JM, Rochitte CE, Dewey M, Arbab-Zadeh A, Niinuma H, Gottlieb I *et al.* Diagnostic performance of coronary angiography by 64-row CT. *N Engl J Med* 2008;**359**:2324–36.
12. Meijboom WB, Van Mieghem CA, van Pelt N, Weustink A, Pugliese F, Mollet NR *et al.* Comprehensive assessment of coronary artery stenoses: computed tomography coronary angiography versus conventional coronary angiography and correlation with fractional flow reserve in patients with stable angina. *J Am Coll Cardiol* 2008;**52**:636–43.
13. Sarno G, Decraemer I, Vanhoenacker PK, De Bruyne B, Hamilos M, Cuisset T *et al.* On the inappropriateness of noninvasive multidetector computed tomography coronary angiography to trigger coronary revascularization: a comparison with invasive angiography. *JACC Cardiovasc Interv* 2009;**2**:550–7.
14. Mahnken AH, Klotz E, Pietsch H, Schmidt B, Allmendinger T, Haberland U *et al.* Quantitative whole heart stress perfusion CT imaging as noninvasive assessment of hemodynamics in coronary artery stenosis: preliminary animal experience. *Invest Radiol* 2010;**45**:298–305.
15. George RT, Jerosch-Herold M, Silva C, Kitagawa K, Bluemke DA, Lima JA *et al.* Quantification of myocardial perfusion using dynamic 64-detector computed tomography. *Invest Radiol* 2007;**42**:815–22.
16. Sorop O, Merkus D, de Beer VJ, Houweling B, Pistea A, McFalls EO *et al.* Functional and structural adaptations of coronary microvessels distal to a chronic coronary artery stenosis. *Circ Res* 2008;**102**:795–803.
17. Duncker DJ, Stubenitsky R, Verdouw PD. Autonomic control of vasomotion in the porcine coronary circulation during treadmill exercise: evidence for feed-forward beta-adrenergic control. *Circ Res* 1998;**82**:1312–22.
18. Bamberg F, Klotz E, Flohr T, Becker A, Becker CR, Schmidt B *et al.* Dynamic myocardial stress perfusion imaging using fast dual-source CT with alternating table positions: initial experience. *Eur Radiol* 2010;**20**:1168–73.
19. Blankstein R, Shturman LD, Rogers IS, Rocha-Filho JA, Okada DR, Sarwar A *et al.* Adenosine-induced stress myocardial perfusion imaging using dual-source cardiac computed tomography. *J Am Coll Cardiol* 2009;**54**:1072–84.
20. Cury RC, Magalhaes TA, Borges AC, Shiozaki AA, Lemos PA, Junior JS *et al.* Dipyridamole stress and rest myocardial perfusion by 64-detector row computed tomography in patients with suspected coronary artery disease. *Am J Cardiol* 2010;**106**:310–5.
21. Rumberger JA, Feiring AJ, Lipton MJ, Higgins CB, Ell SR, Marcus ML. Use of ultrafast computed tomography to quantitate regional myocardial perfusion: a preliminary report. *J Am Coll Cardiol* 1987;**9**:59–69.
22. Bell MR, Lerman LO, Rumberger JA. Validation of minimally invasive measurement of myocardial perfusion using electron beam computed tomography and application in human volunteers. *Heart* 1999;**81**:628–35.
23. Flohr TG, Klotz E, Allmendinger T, Raupach R, Bruder H, Schmidt B. Pushing the envelope: new computed tomography techniques for cardiothoracic imaging. *J Thorac Imaging* 2010;**25**:100–11.

24. Bamberg F, Becker A, Schwarz F, Marcus RP, Greif M, von Ziegler F *et al.* Detection of hemodynamically significant coronary artery stenosis: incremental diagnostic value of dynamic CT-based myocardial perfusion imaging. *Radiology* 2011;**260**:689–98.
25. Bamberg F, Hinkel R, Schwarz F, Sandner TA, Baloch E, Marcus R *et al.* Accuracy of dynamic computed tomography adenosine stress myocardial perfusion imaging in estimating myocardial blood flow at various degrees of coronary artery stenosis using a porcine animal model. *Invest Radiol* 2012;**47**:71–7.
26. Ko BS, Cameron JD, Meredith IT, Leung M, Antonis PR, Nasis A *et al.* Computed tomography stress myocardial perfusion imaging in patients considered for revascularization: a comparison with fractional flow reserve. *Eur Heart J* 2012;**33**:67–77.
27. George RT, Arbab-Zadeh A, Cerci RJ, Vavere AL, Kitagawa K, Dewey M *et al.* Diagnostic performance of combined noninvasive coronary angiography and myocardial perfusion imaging using 320-MDCT: the CT angiography and perfusion methods of the CORE320 multicenter multinational diagnostic study. *AJR Am J Roentgenol* 2011;**197**:829–37.
28. George RT, Arbab-Zadeh A, Miller JM, Vavere AL, Bengel FM, Lardo AC *et al.* Computed tomography myocardial perfusion imaging with 320-row detector computed tomography accurately detects myocardial ischemia in patients with obstructive coronary artery disease. *Circ Cardiovasc Imaging* 2012;**5**:333–40.
29. Kitagawa K, George RT, Arbab-Zadeh A, Lima JA, Lardo AC. Characterization and correction of beam-hardening artifacts during dynamic volume CT assessment of myocardial perfusion. *Radiology* 2010;**256**:111–8.
30. Bastarrika G, Ramos-Duran L, Rosenblum MA, Kang DK, Rowe GW, Schoepf UJ. Adenosine-stress dynamic myocardial CT perfusion imaging: initial clinical experience. *Invest Radiol* 2010;**45**:306–13.
31. Ho KT, Chua KC, Klotz E, Panknin C. Stress and rest dynamic myocardial perfusion imaging by evaluation of complete time-attenuation curves with dual-source CT. *JACC Cardiovasc Imaging* 2010;**3**:811–20.
32. George RT, Arbab-Zadeh A, Miller JM, Kitagawa K, Chang HJ, Bluemke DA *et al.* Adenosine stress 64- and 256-row detector computed tomography angiography and perfusion imaging: a pilot study evaluating the transmural extent of perfusion abnormalities to predict atherosclerosis causing myocardial ischemia. *Circ Cardiovasc Imaging* 2009;**2**:174–82.

IMAGE FOCUS

doi:10.1093/ehjci/jes222
Online publish-ahead-of-print 24 October 2012

Multimodality cardiac imaging in Clozapine-induced eosinophilic constrictive perimyocarditis

Khaled Albouaini, Balazs Ruzsics, and Adrian Chenzbraun*

Department of Cardiology, The Royal Liverpool University Hospital, Prescott Street, Liverpool L7 8XP, UK

* Corresponding author. Tel: +44 (0151) 7063488; fax: +44 (0151) 7065833. Email: a.chenzbraun@btinternet.com

A 21-year-old patient started recently on Clozapine presented with chest pain, ECG changes, eosinophilia, and raised TnT. Echocardiography showed a small pericardial effusion with thickened pericardium and a striking posterolateral echo-bright area, without clear delineation between fibrin clot and subepicardial inflammatory process (*Panel A*). Mitral velocities showed respiratory variations suggestive of constriction (*Panel B*). LV contractility was preserved but longitudinal velocities were reduced (*Panel C*) and borderline values of mitral annular displacement (MAD) by speckle tracking suggested systolic dysfunction (*Panel D*).

Cardiac MRI confirmed mild systolic dysfunction (LVEF = 50%). Contrast enhanced, T1-weighted-delayed enhancement (*Panel E*), delineated high signal intensity band in the pericardium and adjacent epicardium consistent with perimyocarditis with spared endocardium, and mid-myocardium. BTFE cine image (*Panel F*) showed the true relative thickness of the myocardium and the pericardium.

One week after stopping the Clozapine the eosinophilia resolved. Repeat echocardiogram showed no change to the inflammatory features (*Panel G*), but the mitral respiratory variations had disappeared, suggestive of resolving constriction (*Panel H*), and there was normalization of longitudinal velocities (*Panel I*) and MAD (*Panel J*).

The diagnosis of Clozapine myocarditis relies on clinical presentation, imaging, and endomyocardial biopsy. In this case, multimodality imaging was used and allowed the diagnosis of constrictive perimyocarditis. Echocardiography showed pericarditis with a constrictive element and revealed infraclinical myocardial dysfunction consistent with myocarditis. On repeat study, tissue-Doppler and speckle tracking demonstrated that functional recovery before any obvious change in the inflammatory infiltrate was noted. MR confirmed and further refined the diagnosis of perimyocarditis. The agreement and complimentary role of echocardiography and MR were particularly impressive.